

Science with *Herschel*: Results from the HERITAGE project

M. Meixner^{1,2,*}, J. Seale², J. Roman-Duval¹, K. Gordon¹, and the HERITAGE Team

¹ Space Telescope Science Institute, 3700 San Martin Drive, Baltimore, MD 21218, USA

² The Johns Hopkins University, Department of Physics and Astronomy, 366 Bloomberg Center, 3400 N. Charles Street, Baltimore, MD 21218, USA

Received 2014 Apr 7, accepted 2014 Apr 10

Published online 2014 Jun 2

Key words catalogs – dust, extinction – Magellanic Clouds – submillimeter: galaxies – surveys

The *Herschel* Space Observatory completed its last observation on 2013 April 29 after completing 35 000 astronomical observations resulting in numerous discoveries. In this review, we describe the capabilities and general scope of the *Herschel* mission. In particular, we review the science results from one of the open time key programs, the HERschel Inventory of The Agents of Galaxy Evolution (HERITAGE) in the Magellanic Clouds. The HERITAGE project mapped the Large Magellanic Cloud (LMC) and Small Magellanic Cloud (SMC) at 100, 160, 250, 350, and 500 μm using the SPIRE/PACS parallel mode. The total global fluxes for the LMC and SMC agree with measurements by other missions, including Planck. The HERITAGE maps of the LMC and SMC are dominated by the ISM dust emission and bear most resemblance to the tracers of ISM gas rather than the stellar content of the galaxies. The overriding science goal of HERITAGE is to study the life cycle of matter as traced by dust in the LMC and SMC. The far-infrared and submillimeter emission is an effective tracer of the interstellar medium (ISM) dust, the most deeply embedded young stellar objects (YSOs) and the dust ejected by the most massive stars which are discussed briefly in this review. The HERITAGE team has delivered the maps and source catalogs created for each of the 5 bands to the *Herschel* Science Center archive which will hold the legacy of *Herschel*.

© 2014 WILEY-VCH Verlag GmbH & Co. KGaA, Weinheim

1 The *Herschel* Space Observatory

The *Herschel* Space Observatory was an European Space Agency mission with significant contributions from NASA (Fig. 1). On 2009 May 14 *Herschel* was launched together with the Planck mission on an Ariane rocket. *Herschel* cruised to the L2 position and took its first science observation on 2009 September 12. After completing 35 000 astronomical observations resulting in numerous discoveries, the *Herschel* Space Observatory experienced end of helium on 2013 April 29 and ended all science observations. This short review summarizes the *Herschel* Space Observatory capabilities and overall program goals. In the second section, we provide some highlights from the HERschel Inventory of The Agents of Galaxy Evolution (HERITAGE) in the Magellanic Clouds, an open time key program which represents a very small slice of *Herschel*'s science legacy.

1.1 Instruments and capabilities

Herschel was the first space observatory to cover the spectral range of 55–671 μm that covers the far-infrared and submillimeter range and offers views of the “cool” universe (Pilbratt et al. 2010). It had a 3.5 m diameter telescope aperture, which is the largest space telescope flown to date. This large aperture offered improved collecting area and angular



Fig. 1 The *Herschel* Space Observatory shown in a clean room before launch.

* Corresponding author: meixner@stsci.edu

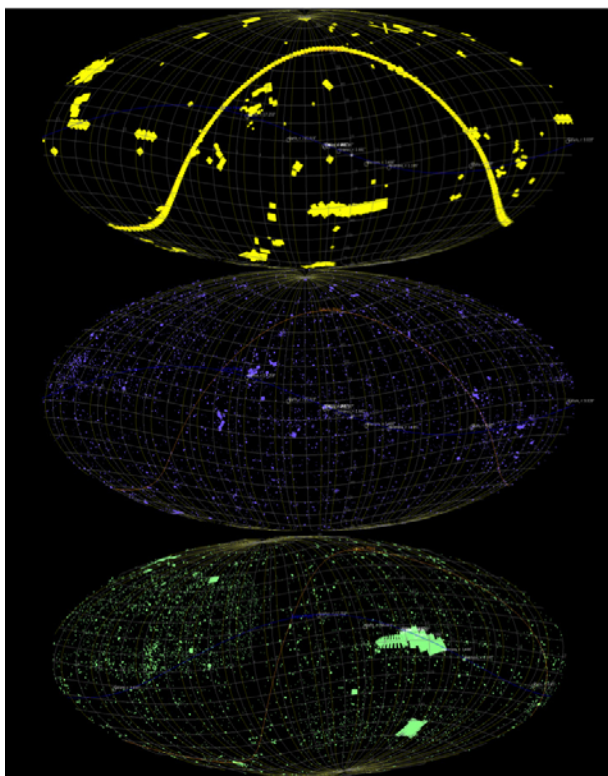


Fig. 2 The sky coverage of the *Herschel* Space Observatory. Top in yellow shows the coverage of the SPIRE/PACS parallel mode. The middle in purple shows the PACS photometry coverage. The bottom in green shows the SPIRE mapping coverage.

resolution over prior observatories. However, the telescope was passively cooled, and the sensitivity of *Herschel* was limited by the warm telescope emission.

With three science instruments, *Herschel* provided wide area mapping in 6 bands, imaging spectroscopy and very high resolution heterodyne spectroscopy. The Photodetector Array Camera and Spectrometer (PACS; Poglitsch et al. 2010) provided broad band imaging at 70, 100, and 160 μm and integral field unit (IFU) spectroscopy that delivered imaging and spectroscopy simultaneously over 51 to 220 μm . The Spectral and Photometric Imaging Receiver (SPIRE; Griffin et al. 2010) provided broad band imaging at 250, 350, and 500 μm and imaging Fourier transform spectrometer (FTS) over the 194–671 μm range. The Heterodyne Instrument for the Far Infrared (HIFI; de Graauw et al. 2010) delivered high spectral resolution spectra, (frequency resolutions of 140, 280, and 560 kHz), using a heterodyne technique over the frequency range of 0.49 to 1.9 THz (615 to 157 μm).

The *Herschel* imaging cameras also provided a facile way to survey large areas of the sky. In particular, the SPIRE and PACS parallel mode of operations permitted 5 band mapping for many of the large key programs. *Herschel* covered $\sim 9.45\%$ of the entire sky during its 23 500 hours of science observing with 6.44% covered by the SPIRE/PACS parallel mode, 2.28% covered by SPIRE photometry and

0.67% covered by PACS photometry (Fig. 2). The spectroscopy, which tends to use a pointed observing strategy is less than 0.08% across the three spectrometers.

1.2 *Herschel* science

Herschel's science program covered all of astronomy. Breaking it down into categories, the observing time on *Herschel* was allocated approximately as 28% on galaxies/active galactic nuclei, 21% on cosmology, 8% on stars/stellar evolution, 39% on the interstellar medium (ISM) and star formation and 4% on solar system. More than half of the *Herschel* observing time went to the key programs.

The science results from *Herschel* are so sweeping and broad that an entire conference with parallel sessions was held at ESTEC in October 2013 to cover them. Although there are no proceedings from this conference the talks are posted on their website¹. There were also two A&A special issues for *Herschel* first results one for PACS and SPIRE and a separate for HIFI, which had a delayed start in operations. These volumes provide the reader with an overview of *Herschel* science. The publication rate of *Herschel* papers is rising and is the fastest after launch compared to other ESA missions. As of the writing of this review, there are 886 papers published.

In this review, we take the approach of discussing some results of HERITAGE, an open time key program of 285 hours, instead of trying to touch on many different results from all the areas of science.

2 HERITAGE

The *Herschel* HERITAGE program mapped the LMC ($8^\circ \times 8.5^\circ$), and SMC ($5^\circ \times 5^\circ$, and $4^\circ \times 3^\circ$) in all SPIRE bands (250, 350, 500 μm) and the 100 and 160 μm PACS bands. The full details of the observational strategy, data reduction processing and creation of the delivered images and catalogs were described by Meixner et al. (2013). The regions of study follow those of the *Spitzer* Surveying the Agents of Galaxy Evolution (SAGE) surveys that covered the wavebands from 3.6 to 160 μm (Meixner et al. 2006; Gordon et al. 2011; Kemper et al. 2011). The HERITAGE data is shown in the 3 color images of the LMC (Fig. 3) and SMC (Fig. 4), and in the global photometry of the spectral energy distributions (SEDs; Fig. 5).

As apparent in all these figures, the emission in the HERITAGE bands is dominated by the ISM dust emission. The images demonstrate that the HERITAGE band emission is distributed in the disks of these galaxies with a network of dusty filaments that make up the ISM. The colors of these images trace the temperature of dust. The bright and white regions are the hottest and tend to be closest to the massive star formation regions. The brightest and largest of these regions is 30 Doradus in the LMC. The greenish yellowish

¹ <http://herschel.esac.esa.int/TheUniverseExploredByHerschel.shtml>

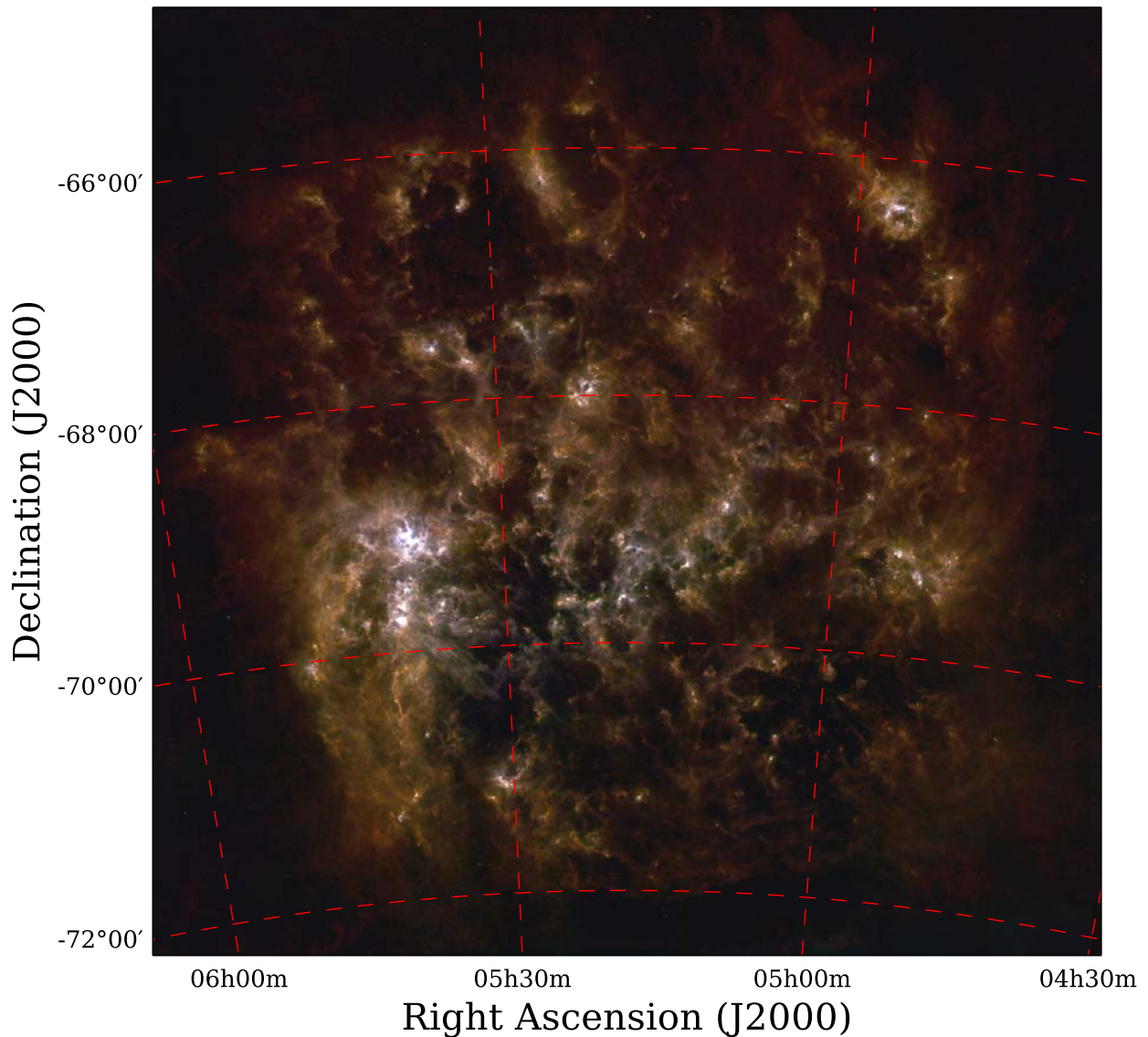


Fig. 3 The LMC HERITAGE data. Red corresponds to SPIRE 250 μm , green to PACS 160 μm , and blue to PACS 100 μm . Figure is from Meixner et al. (2013).

regions are moderate temperature and the reddest regions are the coolest regions.

The global SEDs of the LMC and SMC show the HERITAGE data (Meixner et al. 2013) and the published *Planck* data (Planck collaboration 2011) in comparison to the prior global SED published in the literature. The SED in Fig. 5 shows an improved global flux measurement for the HERITAGE data over the Meixner et al. (2013) paper. Gordon et al. (2014) utilized a better method for subtracting the Milky Way background contribution from the HERITAGE data resulting in the improved measurement. The SEDs feature two peaks. The shorter wavelength peak corresponds to the starlight from these galaxies and the longer wavelength peak arises from the ISM dust emission. Both the *Herschel* HERITAGE data and the *Planck* data arise from the ISM dust emission. We also note that the global fluxes from these two new satellite measurements agrees well with

prior work. The *Herschel* HERITAGE data is new because its superior angular resolution reveals the spatial distribution of these far-infrared and submillimeter emissions for the first time.

In addition to the diffuse ISM dust emission, the HERITAGE data also reveals tens of thousands of compact, dusty sources for which we have created 5 catalogs for the 5 separate spectral bands (Meixner et al. 2013). The 250 micron band is the most sensitive band. Seale et al. (2014) have created a band merged catalog (BMC) of the HERITAGE point source catalogs based on position matching. They extend the matching to shorter wavelengths by position matching to the *Spitzer* SAGE photometry of 3.6, 4.5, 5.8, 8, 24, 70, and 160 μm (Meixner et al. 2006; Gordon et al. 2011). The HERITAGE band merged catalog has 35,304 unique sources for the LMC and 7,531 sources for the SMC.

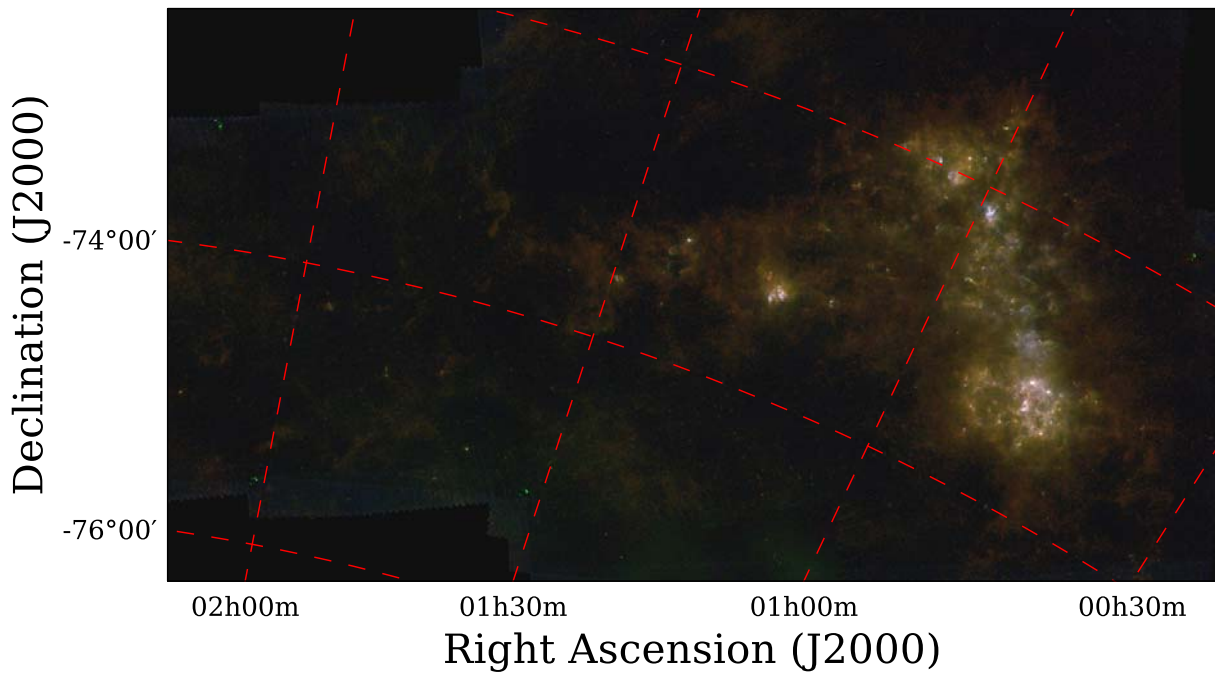


Fig. 4 The SMC HERITAGE data. Red corresponds to SPIRE 250 μm , green to PACS 160 μm , and blue to PACS 100 μm . Figure is from Meixner et al. (2013).

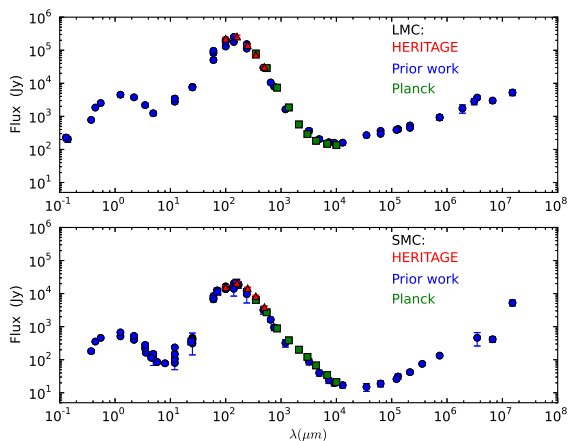


Fig. 5 The spectral energy distributions of the whole LMC and SMC cover the UV to radio wavelengths. Prior work summarized by Israel et al. (2010) includes data from ground and space based missions such as IRAS, DIRBE, TopHat and WMAP. For the SMC, we also include prior work (blue squares) from SAGE-SMC (Gordon et al. 2011). The HERITAGE photometry measured in the PACS and SPIRE bands are shown in red. The *Planck* measurements are shown in green (Planck collaboration 2011).

The scientific goal of HERITAGE is to trace the life cycle of baryonic matter in the LMC and SMC through the dust emission at key transition points. This life cycle starts in the ISM, the mass of which can be traced by the ISM dust emission. Stars form in the densest regions of the ISM and the circumstellar dust of their dense cocoons shines brightly in the far-infrared and submillimeter wavelengths. By find-

ing the young stellar objects (YSOs), one can measure the rate of star formation by counting them (e.g. Whitney et al. 2008; Sewilo et al. 2013). Stars lock up the matter for millions to billions of years, depending on the mass of the star. However, as stars die, they inject metal enriched matter back to the ISM through the dusty winds of asymptotic giant branch (AGB) stars, that are the end stages of intermediate mass stars (e.g. Riebel et al. 2012). Massive dying stars also contribute through the dusty winds of red supergiants (e.g. Sargent et al. 2011) and supernova explosions (e.g. Otsuka et al. 2012; Matsuura et al. 2011). The rates of this metal enrichment can again be quantified by the dust emission from these dying stars. In the next three sections, we highlight results from HERITAGE in these three science areas.

2.1 ISM

The preliminary results on the science demonstration phase (SDP) data from HERITAGE suggested that the ISM dust was different than Milky Way dust (Meixner et al. 2010; Gordon et al. 2010; Galliano et al. 2011). Dust mass maps of the whole LMC and SMC have now been made using just the five bands of the HERITAGE data (Gordon et al. 2014). A few dust models were tried on the data in order to see if the source of excess emission at 500 μm was due to cold dust or to wavelength dependent variations in the dust emissivity. The conclusion is that the “submm excess” is caused by the wavelength dependency of the dust emissivity. Figure 6 shows the spatial distribution in the LMC for the broken emissivity modified blackbody model, which

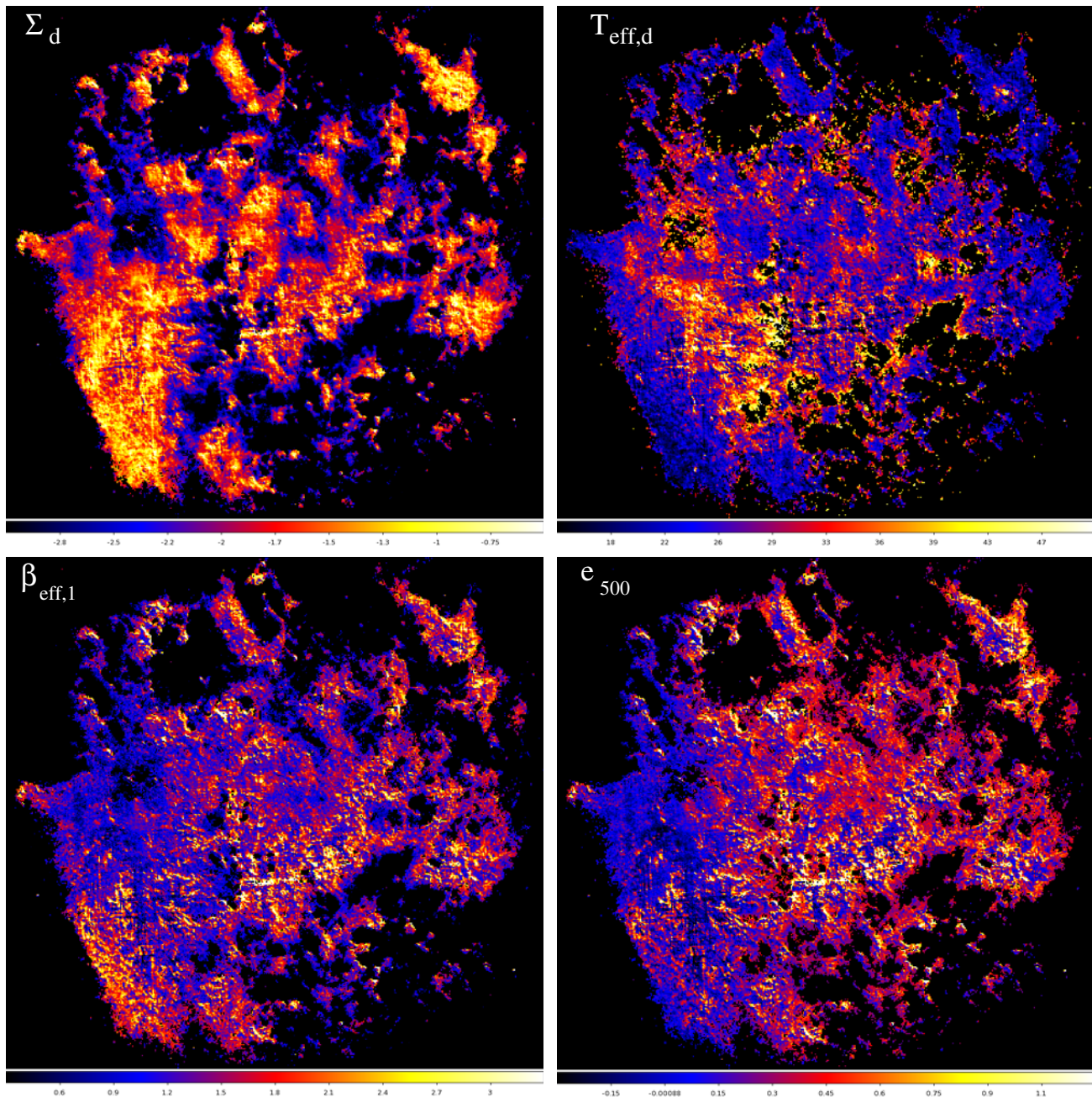


Fig. 6 The LMC’s spatial distribution of the fitted dust parameters for the optimal dust model from Gordon et al. (2014). *From top to bottom, left to right*, this figure shows the Σ_d , the dust mass surface density in $M_\odot \text{pc}^{-2}$; T_d , the dust temperature in K; β_1 , the power-law index for the wavelength dependence of the modified blackbody; and the excess emission at $500 \mu\text{m}$.

was considered the optimal model because it produced more realistic gas-to-dust ratios. The dust mass surface density, Σ_d , shows the variation in the column of dust mass. Gordon et al. (2014) calculate a lower limit to the total mass of dust of 7.3×10^5 and $8.3 \times 10^4 M_\odot$ in the LMC and SMC, respectively.

Roman-Duval et al. (2014) compares these dust mass surface density maps to gas maps created from H I and CO emission from each galaxy. The resulting gas-to-dust mass ratio maps show a spatial variation of this quantity. In particular, the gas-to-dust mass ratio appears to decrease at in-

creasing dust mass column density as shown in Fig. 7 of the SMC. A similar apparent decrease is also observed in the LMC. The correlation of the gas mass and dust mass surface densities is linear in the lowest column density, diffuse atomic gas that is dominated by the H I 21 cm emission. As the dust mass surface density increases beyond $0.04 M_\odot$, the gas mass surface density increases more slowly than linear or “saturates” (Fig. 8). Roman-Duval et al. (2014) offer three possible explanations: 1) Substantial CO-free H_2 gas is unaccounted for in the gas mass. 2) Dust grains coagulate in the denser gas and the emissivity per unit mass of

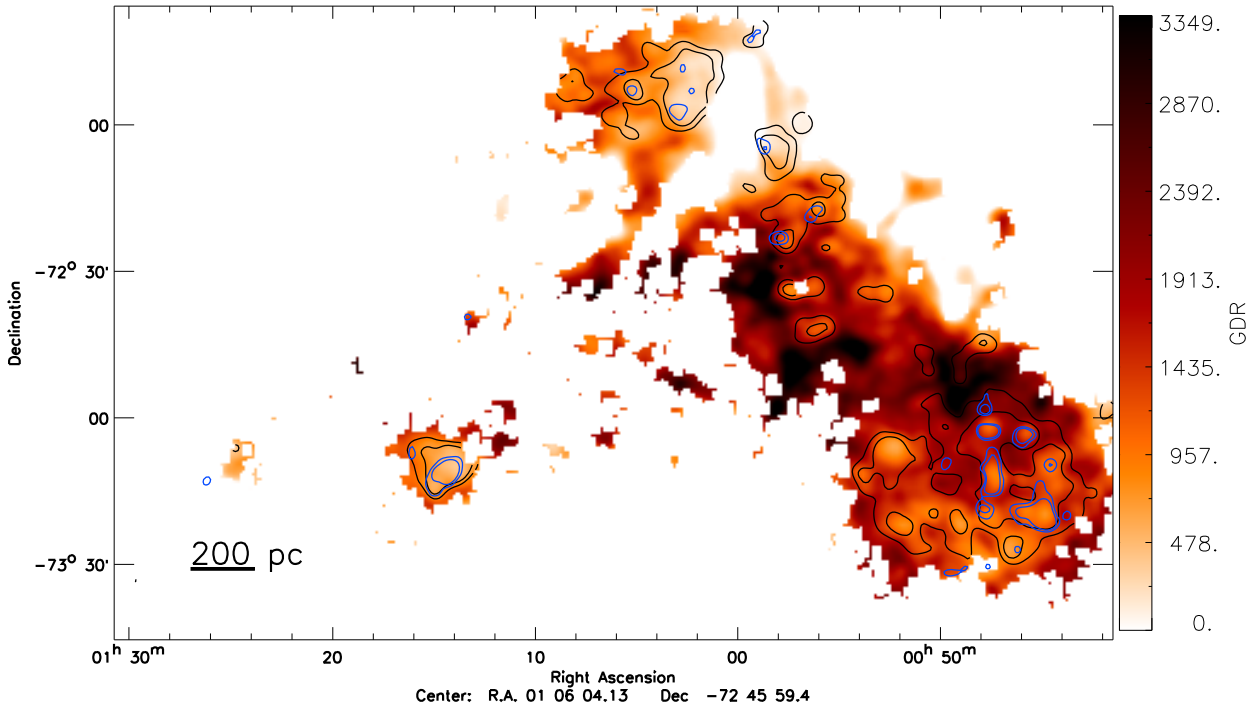


Fig. 7 The SMC's spatial distribution of the gas-to-dust mass ratio from Roman-Duval et al. (2014). The black contours show the 0.02 and 0.03 $M_{\odot} \text{pc}^{-2}$ levels of dust mass surface density. The blue contours trace the 0.5 and 0.8 K km s^{-1} level of the CO integrated intensity from Mizuno et al. (2001).

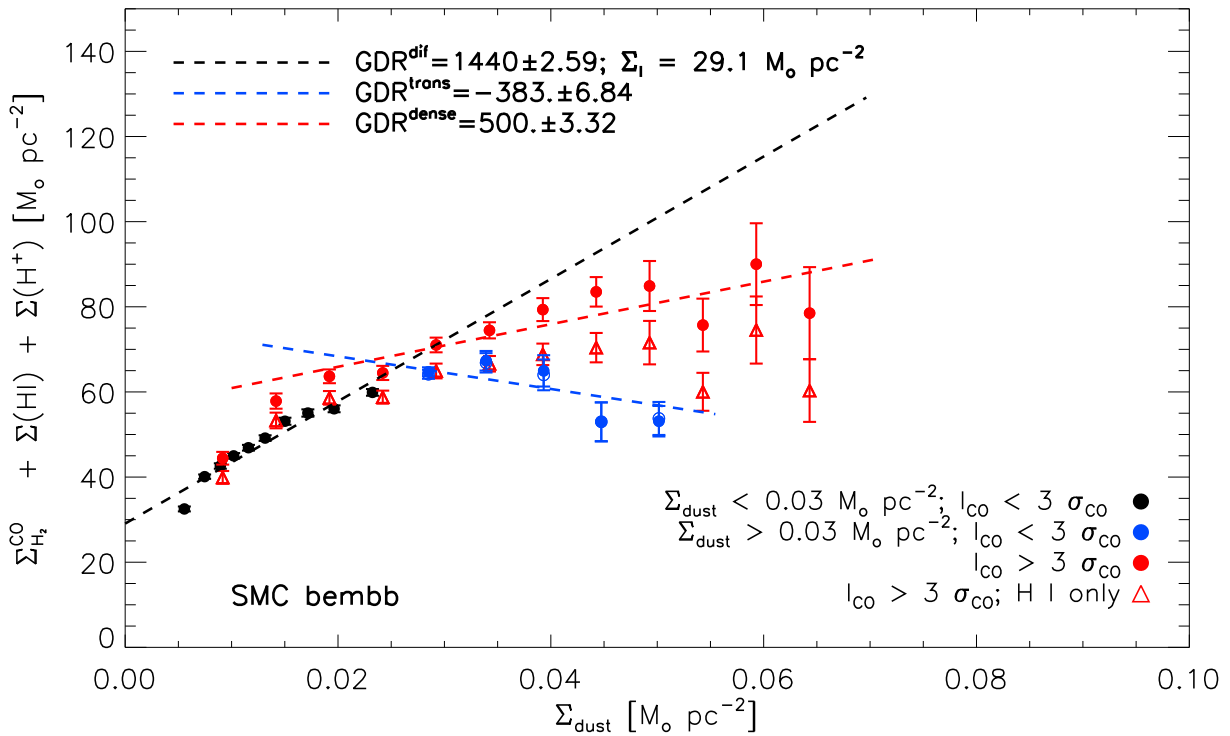


Fig. 8 The pixel-to-pixel correlation between dust and gas surface densities in the SMC from Roman-Duval et al. (2014). The slope of the dust/gas relation corresponds to the gas-to-dust mass ratio and decreases as surface density increases. The black, blue and red colors correspond to three different groups of pixels. Diffuse atomic gas is shown as black points including pixels with $\Sigma_{\text{dust}} \leq \Sigma_{\text{d}}^{\text{dif}}$ and no detectable CO emission (below the $3\sigma_{\text{CO}}$ noise level). Translucent molecular and atomic gas mixture is represented by blue points corresponding to pixels with $\Sigma_{\text{dust}} \geq \Sigma_{\text{d}}^{\text{dif}}$ and no CO emission. Molecular gas is represented by red points that are associated with pixels with CO emission above the $3\sigma_{\text{CO}}$ noise level.

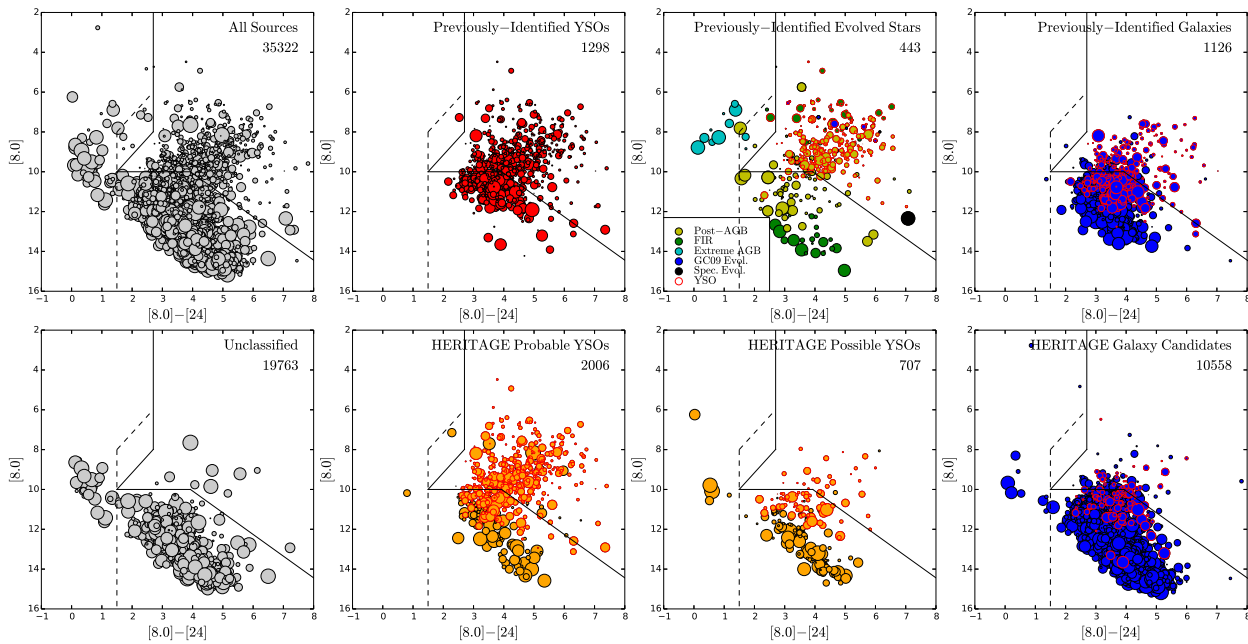


Fig. 9 The $[8.0]$ vs. $[8.0] - [24]$ color-magnitude diagram for the HERITAGE band merged catalog of the LMC from Seale et al. (2014). The *top left* panel shows all the sources with 8.0 and 24 μm counterparts. The remaining panels show different classified populations. The *top row* shows previously-identified sources while the *bottom row* shows new classifications from Seale et al. The number of sources in that population is listed below the name. Previously classified YSOs are outlined in red in all panels.

the dust changes. Because our dust mass analysis does not take this into account, we overestimate the dust mass in the dense regions and in fact the gas-to-dust mass ratio is constant. 3) Dust grains really do accrete elements from the gas phase and their mass increases in the dense phases resulting in a real decrease of the gas-to-dust mass ratio. They suggest that all three processes may be required to account for the apparent gas-to-dust ratio changes.

2.2 Star formation and YSOs

The HERITAGE SDP data demonstrated that we could both analyze the environments of known massive star formation regions like N44 (Hony et al. 2010) and also discover the earliest stages of star formation, the Class 0 YSOs, in the Magellanic Clouds (Sewiło et al. 2010). Whole galaxy wide searches for star formation sites with HERITAGE has been completed by Seale et al. (2014). The band merged catalog of HERITAGE sources has been characterized as either YSOs, background galaxies or dusty remnants of stellar death. Using the *Herschel* Atlas survey (Eales et al. 2010) as a comparison, Seale et al. (2014) determined the most point like sources in the HERITAGE catalogs were background galaxies: ~ 9700 in the LMC and ~ 5100 in the SMC. The next dominant population of sources are the YSO candidates with ~ 3500 in the LMC and ~ 660 in the SMC. In the LMC 73% and in the SMC 35% of these YSOs are newly-identified.

Not all the HERITAGE sources have *Spitzer* SAGE counterparts, but many of the classified sources do. Figure 9 shows the LMC $[8]$ vs. $[8] - [24]$ color-magnitude di-

agram (CMD) for HERITAGE band merged catalog in the LMC as presented by Seale et al. (2014). The previously identified sources such as YSOs, evolved stars and galaxies were determined by *Spitzer* SAGE and in some cases by spectroscopic confirmation. We note that there is overlap in the previously-identified lists of candidate populations which emphasizes the fact that these are candidates and followup of these sources is required for confirmation. The newly identified YSOs by Seale et al. (2014) tend to be fainter sources in the $[8]$ vs. $[8] - [24]$ CMD which may be due to their highly embedded nature. The HERITAGE background galaxies are significantly larger in number than previously identified galaxies and are all on the fainter end of the CMD. The evolved star population is much smaller in number, ~ 400 , and are discussed in the next section.

2.3 Evolved stars and SN1987A

Only very dusty and luminous evolved stars are expected to be detected in the HERITAGE survey. Hence, it is not entirely clear that all of the ~ 400 LMC and ~ 50 SMC evolved star candidates from Seale et al. (2014) are really evolved stars given that many have other identifications such as YSOs. However, detailed investigations of a few evolved stars based on the SDP data show that at least two massive evolved stars (R71 and IRAS05280–6910) have HERITAGE detections (Boyer et al. 2010). More detailed followup on these other evolved star candidates will be needed.

In addition to the stellar winds, dust can be produced by the supernovae explosions. The supernova remnant, N49,

was clearly detected in the HERITAGE SDP data. Otsuka et al. (2010) estimated a large, cold dust mass ($10 M_{\odot}$) associated with N49. However, most of this mass is associated with a molecular cloud into which N49 is colliding. Quite surprisingly, we detected SN 1987A in the full HERITAGE data set. We were surprised by this detection because extrapolations of SN 1987A's SED based on *Spitzer* data predicted that it would fall below our *Herschel* detection limit. For that reason, we did not even mention SN 1987A in our original, pre-launch HERITAGE proposal. It is a demonstration of *Herschel's* superior angular resolution over prior facilities that enabled this spectacular discovery.

Matsuura et al. (2011) reported the SN 1987A detection by the HERITAGE survey at 100, 160, 250, and 350 μm . They interpreted the detection as 0.4–0.7 M_{\odot} of dust associated with the explosive ejecta of SN 1987A. This remarkable detection is the first to detect so much dust mass from a supernova explosion. It supports theoretical suggestions that supernovae explosions produce much of the dust for the dusty high- z galaxies. Recent ALMA observations spatially resolve the sub-millimeter dust emission to be clearly associated with the supernova explosion (Indebetouw et al. 2014). ALMA (Kametsky et al. 2013) and followup *Herschel* observations (Matsuura et al. 2014) reveal some CO molecular gas emission, but contamination of the continuum emission is less than 8%.

3 *Herschel* lives on

Although, *Herschel* has lost its helium and is no longer taking observations, it will live on for decades and perhaps a century. The legacy of the *Herschel* mission is its science archive². Improved data products from the HERITAGE project and many other Key programs have delivered or will soon deliver their data to the *Herschel* Science Archive.

Acknowledgements. Margaret Meixner thanks Thomas Rauch and Klaus Werner for inviting her to speak at the Astronomische Gesellschaft Tübingen 2013 meeting. Goran Pilbratt provided information on the *Herschel* mission included in this paper. We acknowledge financial support from the NASA *Herschel* Science Center, JPL contracts #1381522, 1381650, and 1350371. We thank the contributions and support from the European Space Agency (ESA), the PACS and SPIRE teams, the *Herschel* Science Center and the NASA *Herschel* Science Center and the PACS and SPIRE instrument control centers, without which none of this work would be possible. Finally, we acknowledge that the HERITAGE key program represents the results from a large team of scientists, all of whom are noted as co-authors in the Meixner et al. (2013) overview paper.

References

- Boyer, M. L., Sargent, B., van Loon, J. T., et al. 2010, *A&A*, 518, L142
- de Graauw, T., Helmich, F. P., Phillips, T. G., et al. 2010, *A&A*, 518, L6
- Eales, S., Dunne, L., Clements, D., et al. 2010, *PASP*, 122, 499
- Galliano, F., Hony, S., Bernard, J.-P., et al. 2011, *A&A*, 536, A88
- Gordon, K. D., Galliano, F., Hony, S., et al. 2010, *A&A*, 518, L89
- Gordon, K. D., Meixner, M., Meade, M. R., et al. 2011, *AJ*, 142, 102
- Gordon, K. D., Roman-Duval, J., Bot, C., et al. 2014, *ApJ*, *in press*
- Griffin, M. J., Abergel, A., Abreu, A., et al. 2010, *A&A*, 518, L3
- Hony, S., Galliano, F., Madden, S. C., et al. 2010, *A&A*, 518, L76
- Indebetouw, R., Matsuura, M., Dwek, E., et al. 2014, *ApJL*, *in press*
- Kamenetzky, J., McCray, R., Indebetouw, R., et al. 2013, *ApJL*, 773, L34
- Kemper, F., Woods, P. M., Antoniou, V., et al. 2010, *PASP*, 122, 683
- Matsuura, M., Dwek, E., Meixner, M., et al. 2011, *Science*, 333, 1258
- Matsuura, M., Dwek, E., Barlow, M. J., et al. 2014, *ApJL*, *in press*
- Meixner, M., Gordon, K., Indebetouw, R., et al. 2006, *AJ*, 132, 2268
- Meixner, M., Galliano, F., Hony, S., et al. 2010, *A&A*, 518, L71
- Meixner, M., Panuzzo, P., Roman-Duval, J., et al. 2013, *AJ*, 146, 62
- Mizuno, N., Rubio, M., Mizuno, A., et al. 2001, *PASJ*, 53, L45
- Otsuka, M., van Loon, J. T., Long, K. S., et al. 2010, *A&A*, 518, L139
- Otsuka, M., Meixner, M., Panagia, N., et al. 2012, *ApJ*, 744, 26
- Pilbratt, G. L., Riedinger, J. R., Passvogel, T., et al. 2010, *A&A*, 518, L1
- Planck Collaboration, Ade, P. A. R., Aghanim, N., et al. 2011, *A&A*, 536, A17
- Poglitsch, A., Waelkens, C., Geis, N., et al. 2010, *A&A*, 518, L2
- Riebel, D., Srinivasan, S., Sargent, B., & Meixner, M. 2012, *ApJ*, 753, 71
- Roman-Duval, J., Gordon, K. G., Meixner, M., et al. 2014, *ApJ*, *in press*
- Sargent, B. A., Srinivasan, S., & Meixner, M. 2011, *ApJ*, 728, 93
- Seale, J., Meixner, M., Sewilo, M., et al. 2014, *ApJ*, *in press*
- Sewilo, M., Indebetouw, R., Carlson, L. R., et al. 2010, *A&A*, 518, L73
- Sewilo, M., Carlson, L. R., Seale, J. P., et al. 2013, *ApJ*, 778, 15
- Whitney, B. A., Sewilo, M., Indebetouw, R., et al. 2008, *AJ*, 136, 18

² http://herschel.esac.esa.int/Science_Archive.shtml